

Impurity behavior during ICRH and NBI operation with ITER-like wall at JET

A. Czarnecka¹, V. Bobkov², I. H. Coffey³, P. Jacquet⁴, C. C. Klepper⁵, K. D. Lawson⁴,
E. Lerche⁶, C. F. Maggi², M.-L. Mayoral⁴, T. Pütterich², D. Van Eester⁶
and JET-EFDA contributors*

*JET-EFDA, Culham Science Centre, Abingdon, OX14 3DB, UK, ¹Institute of Plasma Physics and Laser Microfusion, Association EURATOM-IPPLM, Hery 23 Str., 01-497 Warsaw, Poland, ²Max-Planck-Institut für Plasmaphysik, EURATOM-Assoziation, D-85748 Garching, Germany, ³Department of Physics, Queen's University, Belfast, BT7 1NN, Northern Ireland, UK, ⁴Euratom/CCFE Association, Culham Science Centre, Abingdon, OX14 3DB, U, ⁵Oak Ridge National Laboratory, Oak Ridge, TN 37831-6169, USA, ⁶Association "EURATOM - Belgian State", ERM-KMS, TEC Partner, Belgium, *See the Appendix of F. Romanelli et al., Fusion Energy Conference 2010 (Proc. 23rd Int. Conf. Daejeon, Korea, 2010) IAEA, (2010)*

INTRODUCTION

Magnetically confined plasmas, such as those produced in the tokamak JET, contain measurable amounts of impurity ions produced during plasma-wall interactions (PWIs). The impurities including high- and mid-Z elements need to be controlled within tolerable limits, to ensure they do not significantly affect the performance of the plasma. This contribution focuses on documenting the nickel (Ni) behavior in the plasma during Ion Cyclotron Resonance Heating (ICRH) and comparing the Ni levels during operation with the ITER-Like wall (ILW) that consists of a tungsten (W) divertor and a beryllium (Be) main wall, with levels during operation with the previous Carbon (C) wall. Ni release during ICRH is presented as a function of the applied power level, relative phasing of the antenna straps, plasma-strap distance, different plasma configuration and compared with release during Neutral Beam Injection (NBI).

EXPERIMENTAL ARRANGEMENT

JET has an ICRH system with four A2 antennas, known as A, B, C and D and one "ITER-like" antenna (not used in 2011). Each A2 antenna is a phased array of 4 toroidal straps. The Faraday screens bars facing the plasma are made of beryllium and the surfaces of the antenna housing and central conductors are coated with Ni. Note that that antennas A and B are connected via 3dB splitters and are operated simultaneously and that only half of antennas A and B (A12 and B12) were used for this study. Spectroscopic measurements along the vessel midplane were obtained using the SPRED (survey poor resolution extended domain) spectrometer with the routinely used 450 gmm⁻¹ holographic grating. This registers the VUV spectra in the wavelength range 100–1100 Å. With the former carbon PFCs the VUV spectrum was dominated by different mid-Z metallic impurities like nickel, iron, chromium and copper [1]. Note that with the Be/W, the spectrum also contained intense W features. Since in the low temperature plasma, below $T_e(0) = 2$ keV, the Ni XVIII ions are localized close to the plasma core, the normalization of signals to the square of the local line integrated density becomes a reasonable measure of the impurity content in the plasma core. When the higher Ni ionization stages were present in the plasma, the determination of Ni impurity densities, based on the combination of absolutely calibrated VUV line transition intensity measurements with the Universal Transport Code (UTC) simulations is described in details in [1].

EXPERIMENTAL RESULTS

In the experiments reported here, dipole ($0 \pi 0 \pi$) and -90° ($0 -\pi/2 -\pi -3\pi/2$) antenna phasings were used, corresponding to symmetric (dominant $k_{||} \sim 6.6 \text{ m}^{-1}$) and asymmetric (countercurrent, dominant $k_{||} \sim 3.3 \text{ m}^{-1}$) wave spectrum, respectively. The ICRH scheme used

was Hydrogen minority in D plasmas using an ICRH frequency of 42 MHz. The first set of experiments was performed in L-mode with the magnetic field strength $B_T=2.4$ T, the plasma current ranging from 1.4 to 2.4 MA and a plasma separatrix - outer limiter distance in the midplane (ROG) in the range of 3 to 6 cm, with 1 MW of power level per antenna

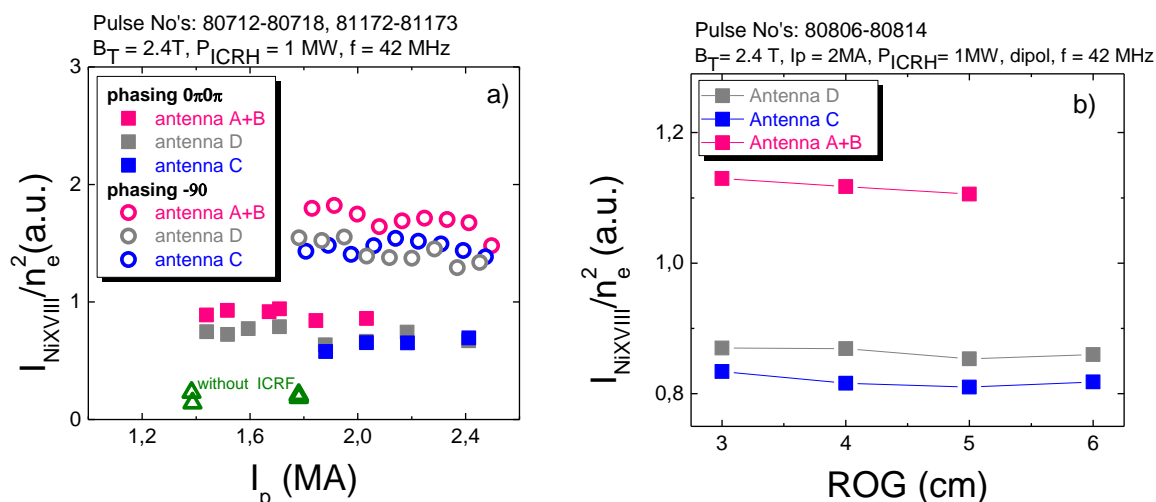


Fig. 1. Correlation between Ni content and a) I_p scan for 2 different antenna phasing b) limiter-separatrix distance ROG to individual ICRF antennas.

As illustrated on Fig.1a, not dependence is observed with the plasma current but for the same ICRH power level, -90° phasing gives a significant higher Ni concentration than in the case of dipole phasing. This result is similar to the ones obtained in the previous campaigns at JET with C wall where for antenna phasings with higher dominant $k_{||}$, the Ni impurity concentration was reduced in the central part of the plasma [2]. A similar impact of antenna phasing was observed in the enhanced release of W [3] and Be [4] and points to radio frequency (RF) sheaths [5] effects. Indeed, ions accelerated in the sheaths voltage surrounding the ICRH antennas can lead to enhanced sputtering of magnetically connected surfaces and additional heat loads [6]. No obvious dependence is seen during ROG variation (see Fig. 1b). As seen on both Fig.1, the Ni content is less pronounced during the operation of antenna C and D than during A+B operation although the same total power level was coupled. This can be due to differences in antenna spectrum (for A and B only 2 over 4 straps are powered) that could results in higher high antenna near fields and higher surface of interaction (two antennas are used).

Fig. 2a shows that the Ni concentration increases with the ICRH power and for the same NBI power level, ICRH-heated plasmas are characterized by higher Ni content. This comparison is made at the same edge electron density, $n_e=2\times 10^{19}$ m⁻³. Similar results are found in low power H-mode discharges and in limiter configurations. Additionally in ICRH and NBI discharges, the influence of the variations in divertor configuration and main plasma shape by changes in upper δ_U (from ~ 0.2 to ~ 0.4) and lower δ_L (from ~ 0.3 to ~ 0.4) triangularity on the Ni content was investigated with the ILW. The main purpose of the experiment was to study the influence of the ILW on the L-H power threshold [7]. Fig.2a shows dependence of Ni content on plasma configuration with measurement time of 0.5 s before L-H transition, for high triangularity shapes referred as HT3L, HT3R, HT3 and low triangularity shapes referred as V5 and V5L (the letter L, R refer to different outer strike point positions). The Ni content decreased with increasing line averaged edge plasma density, measured by interferometry at the radial location 3.7 m (see Fig. 3b), also increased with plasma triangularity (see Fig. 2c).

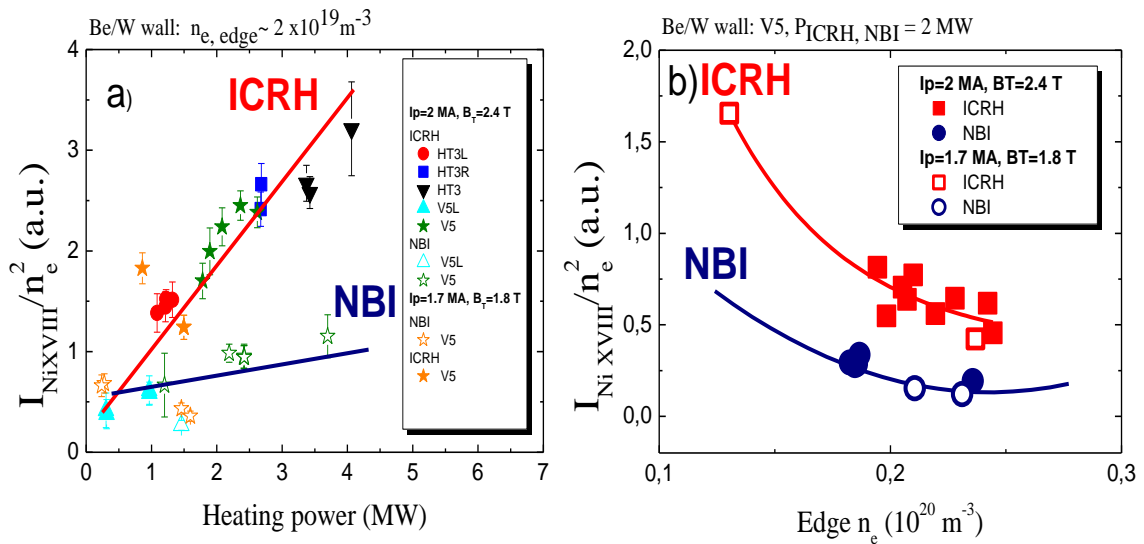
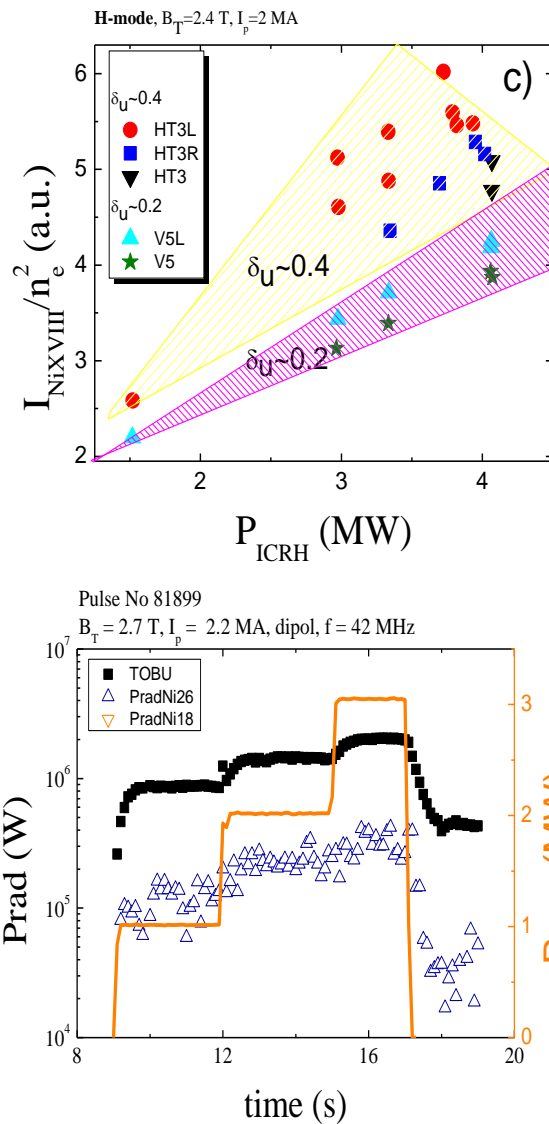


Fig. 2 Dependence of Ni content on plasma configuration measured at L-H transition, $B_T = 2.4 \text{ T}$, $I_p = 2 \text{ MW}$, for high and low triangularity shapes with ICRH and NBI heated plasma vs. a) heating power, b) edge density, and c) power ICRH in H-mode.



As larger Ni and W concentrations [3] are measured with ICRH than with NBI heating, not surprisingly higher bulk radiated power ($P_{\text{rad,bulk}}$) is measured when using ICRH compared to NBI [8]. The contribution of Ni to $P_{\text{rad,bulk}}$ was evaluated based on calculations of the Ni cooling factor presented in [9]. It was observed that although with the new Be/W metal wall the main radiation came from W, Ni was also contributing significantly to $P_{\text{rad,bulk}}$ up to a 20 % level during ICRH, depending on the plasma conditions. Example is shown in Fig.3.

Fig. 3 Contribution of Ni to $P_{\text{rad,bulk}}$ during ICRF heating.

For the same power level, central ICRH resulted in higher Ni concentration in the plasma core in comparison to off-axis ICRH as is shown in Fig. 4. This effect can be due to the higher central T_e and diamagnetic energy observed with on-axis heating (Fig.5), difference

in transport or higher Ni influx. The effect of the temperature is shown by the open symbols in Fig.4, which represent the Ni concentration for the on-axis case computed with the same temperature as the off-axis case

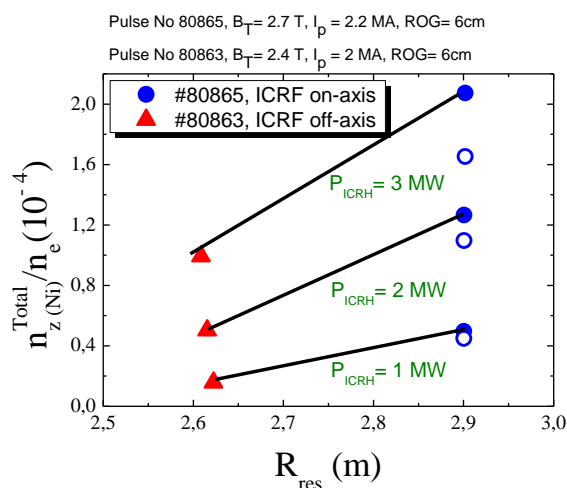


Fig. 4 Correlation between Ni concentration [1] and the resonance minority cyclotron resonance position. Open symbols represent the Ni concentration for the on-axis case computed with the same temperature as the off-axis case.

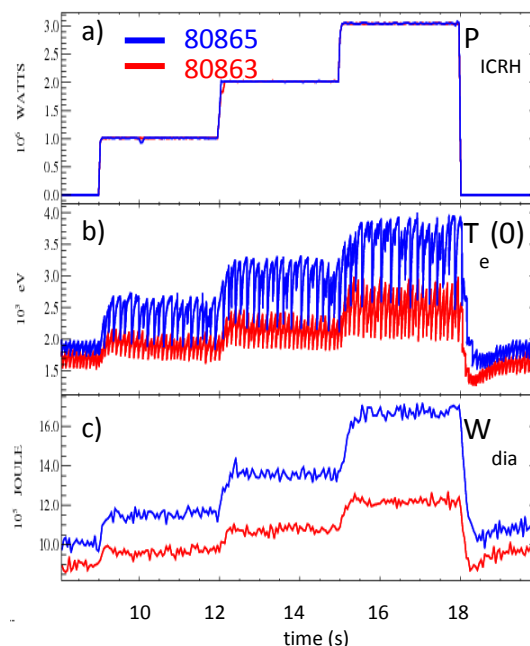


Fig. 5 Time traces of a) ICRH power, b) central electron temperature, c) diamagnetic energy for on-axis (Pulse No 80865) and off-axis (Pulse No 80863) ICRH

SUMMARY

A variety of plasma wall interactions (PWIs) during operation of the auxiliary heating systems is observed in JET with the ITER-like wall. The application of ICRF power results in higher Ni content in the plasma core compared with NBI heating, in both L- and low power H-mode discharges, in divertor and limiter configurations. Differences in plasma wall–interaction for the different plasma shape, antenna phasing, plasma-antenna distance, and the minority cyclotron resonance position shown constitute another factor influencing impurity release.

ACKNOWLEDGMENTS

This work was supported by EURATOM and carried out within the framework of the European Fusion Development Agreement. The views and opinions expressed herein do not necessarily reflect those of the European Commission.

REFERENCES

- [1] A. Czarnecka et al. Plasma Phys. Control. Fusion **53** (2011) 035009
- [2] A. Czarnecka et al. Plasma Phys. Control. Fusion **54** (2012) 074013
- [3] V. Bobkov, Proc. 20th Int. Conf. on PSI, 21-25 May 2012, Aachen, Germany, O3
- [4] C. C. Klepper, Proc. 20th Int. Conf. on PSI, 21-25 May 2012, Aachen, Germany, P1-86
- [5] D. A. D’Ippolito and J.R. Myra, *Journal of Nuclear Materials* **415** (2011) S1001
- [6] Ph. Jacquet, Proc. 20th Int. Conf. on PSI, 21-25 May 2012, Aachen, Germany, P1-20
- [7] C. F. Maggi et al., this conference
- [8] D. Van Eester et al., this conference
- [9] D. Post et al. At. Data Nucl. Data Tables **20** (1977) 397